

# Model-based Deep Learning for Rate Split Multiple Access in Vehicular Communications

Hanwen Zhang\*, Mingzhe Chen<sup>†</sup>, Alireza Vahid<sup>‡</sup>, Haijian Sun\*

\*School of Electrical and Computer Engineering, University of Georgia, Athens, GA, USA

<sup>†</sup>Department of Electrical and Computer Engineering, University of Miami, Coral Gables, FL, USA

<sup>‡</sup>Electrical and Microelectronic Engineering, Rochester Institute of Technology, Rochester, NY, USA

Emails: hanwen.zhang@uga.edu, mingzhe.chen@miami.edu, arveme@rit.edu, hsun@uga.edu

**Abstract**—Rate split multiple access (RSMA) has been proven as an effective communication scheme for 5G and beyond, especially in vehicular scenarios. However, RSMA requires complicated iterative algorithms for proper resource allocation, which cannot fulfill the stringent latency requirement in resource constrained vehicles. Although data driven approaches can alleviate this issue, they suffer from poor generalizability and scarce training data. In this paper, we propose a fractional programming (FP) based deep unfolding (DU) approach to address resource allocation problem for a weighted sum rate optimization in RSMA. By carefully designing the penalty function, we couple the variable update with projected gradient descent algorithm (PGD). Following the structure of PGD, we embed few learnable parameters in each layer of the DU network. Through extensive simulation, we have shown that the proposed model-based neural networks has similar performance as optimal results given by traditional algorithm but with much lower computational complexity, less training data, and higher resilience to test set data and out-of-distribution (OOD) data.

**Index Terms**—RSMA, model-based deep learning, deep unfolding, projection gradient descent, low complexity, fractional programming

## I. INTRODUCTION

Rate split multiple access (RSMA) is a cutting-edge multiple access technique in future wireless communication systems [1]–[6]. RSMA divides the data stream into a common part, which conveys information shared by multiple users, and a private part to fulfill individual user requirements. This scheme efficiently utilizes spectrum resources by broadcasting the common information, thereby freeing up bandwidth for private data, which can improve individual quality-of-service (QoS). [3] derived a closed-form solution for the optimal private beamformer and showed that RSMA has advantages in resource allocation tasks with a massive number of users, minimum rate demand of users, and low transmit power scenarios. Besides, it also provided a basic scheme for resource allocation in single-input single-output RSMA systems. Moreover, RSMA is a promising solution in vehicular communications, where the common message is critical safety information and private messages reflect each vehicle’s control data. [1], [2], [7] have demonstrated RSMA robustness, especially in scenarios with high latency sensitivity, which is essential in vehicular communications. To reduce system latency in vehicular communications, the lower computational workload is also required. Following this, there are some results focused on

low complexity algorithms [5], [6]. Specifically, in [5], the authors proposed a low complexity algorithm by reducing the redundant constraints and pre-processing deployment region modeling. [6] designed zero forcing (ZF) and maximum ratio transmission (MRT) based methods to find closed-form expression solution for the RSMA max-min fairness problem and reduce computational complexity. However, given the higher mobility and stringent latency demands in vehicle communication, the low complexity algorithms given above are still hard to meet the requirements.

Deep learning has emerged as a pivotal approach to enhance the performance of communication systems [8], [9]. Leveraging large datasets, deep learning facilitates the development of neural network models that are capable of learning from data without explicit expressions [10]. However, the mappings learned during the training process often yield unpredictable outcomes when exposed to out-of-distribution (OOD) scenarios, which is caused by the lack of explicit physical principles constraints [11]. To solve this problem, large amount of data is required to train a model that is able to make neural networks robust in OOD scenarios. As a result, model-based deep learning is considered a promising alternative to problems where the paradigm incorporates domain knowledge to design an interpretable neural network architecture. It enables the training of neural networks with less data while achieving robust performance in OOD [11]. Model-based deep learning integrates interpretable models into deep learning architectures, enhancing their applicability to complex problems [11]. In the context of wireless resource allocation, several studies have proposed learning-based optimization strategies. For instance, [12] presents a graph convolution network weighted minimum mean square error (GCN-WMMSE) deep unfolding (DU) algorithm that combines GCNs with WMMSE method to achieve robust neural networks based resource allocation. Meanwhile, [13] adopts Uzawa’s method [14] to integrate constraint-related variables with the objective function for DU network design. The particularly relevant work is [15], which extends the approach to general scenarios, using a fractional programming (FP) based DU framework to tackle the weighted sum rate (WSR) problem in RIS scenario. In our research, we focus on resource allocation scenarios with a more general FP framework and also tackle the problem with variables that do

not appear in the objective function. Moreover, the specially designed learnable parameters can specifically enhance robustness in OOD test with much lower complexity.

To address the challenges in designing model-based deep learning networks for wireless resource allocation in multiple-input single-output (MISO) RSMA scenarios, we introduce a FP based DU framework. This framework is applicable to various resource allocation problems. We summarize the contributions of this paper as follows:

- We address a classic multi-user MISO RSMA resource allocation utilizing FP, which offers a versatile framework suitable for a variety of optimization problems, particularly fractional programming. This FP-based approach enhances flexibility for application in complex RSMA scenarios, including those focused on energy efficiency and fairness-oriented optimization.
- We extend FP framework by applying the projected gradient descent (PGD) algorithm and unfolding structure. To address the updating problem of variables that only exist in the constraint, we introduce a specially designed penalty factor to update the common stream beamformer in PGD. Subsequently, to boost the algorithm performance, we design a DU-based interpreted learning framework with only few learnable parameters in each layer.
- Finally, the experiments provide a comprehensive analysis on the convergence and the optimal hyper-parameters comparison to show proposed algorithm has similar performance as traditional optimization. Then, we provide the OOD test result to validate that the structure we designed is robust in different environments. The last experiment shows the proposed model has much lower computational complexity than traditional algorithms. The provided experiments sufficiently show model-based solution has the potential for wireless resource allocation optimization.

Notation: We use bold capital symbol as matrix, bold lowercase symbol as vectors, the lowercase symbol as scalar,  $\|\cdot\|$  as  $l_2$  norm,  $\text{Re}\{\cdot\}$  as real part of function,  $[\cdot]^H$  as Hermite transpose,  $[\cdot]^T$  as transpose,  $\mathcal{U}\{\cdot\}$  as uniform distribution,  $\mathcal{N}\{\cdot\}$  as Gaussian distribution,  $\bar{z}$  as conjugate of  $z$ .

## II. SYSTEM MODEL AND PROBLEM FORMULATION

### A. System Model

We consider a downlink vehicular communication system, which consists of a single base station (BS) or roadside unit (RSU) with  $M$  antennas and a total of  $U$  single-antenna vehicular users (VUs). In an RSMA system, data is split into common and private streams. The common stream embeds messages for all VUs (eg., critical safety information) while the private stream provides individual data for each VU. Denote  $\mathbf{v}_0, \mathbf{v}_k \in \mathbb{C}^{M \times 1}$  the beamforming vectors for common and private data streams, respectively. The BS transmit signal for common stream and VU  $k$  private stream are given by:

$$\mathbf{x}_0 = \mathbf{v}_0 s[n], \quad (1)$$

$$\mathbf{x}_k = \mathbf{v}_k s_k[n], k \in \{1, 2, \dots, U\}, \quad (2)$$

where  $s[n]$  and  $s_k[n]$  are the common and dedicated data streams, respectively.  $E(s[n])^2 = E(s_k[n])^2 = 1$ , i.e., both data streams are normalized. The received signal of VU  $k$  is:

$$y_k = \mathbf{h}_k^H \mathbf{x}_k + \mathbf{h}_k^H \mathbf{x}_0 + \sum_{j \neq k} \mathbf{h}_k^H \mathbf{x}_j + n_k, \quad (3)$$

where  $\mathbf{h}_k \in \mathbb{C}^{M \times 1}$  is the channel between BS and VU  $k$ , which follows circularly symmetric complex Gaussian distribution with power  $h_k$ ,  $\mathbf{h}_k \sim \mathcal{CN}(\mathbf{0}, h_k^2 \mathbf{I})$ .  $n_k \sim \mathcal{N}(0, \sigma_k^2)$  is AWGN noise. The achievable common stream data rate of VU  $k$  is given below in (4), while the private stream is given as (5):

$$c_k = \log_2 \left( 1 + \frac{\mathbf{h}_k^H \mathbf{v}_0 \mathbf{v}_0^H \mathbf{h}_k}{\sigma_k^2 + \sum_{j=1}^U \mathbf{h}_k^H \mathbf{v}_j \mathbf{v}_j^H \mathbf{h}_k} \right), \quad (4)$$

$$R_k^p = \log_2 \left( 1 + \frac{\mathbf{h}_k^H \mathbf{v}_k \mathbf{v}_k^H \mathbf{h}_k}{\sigma_k^2 + \sum_{j \neq k} \mathbf{h}_k^H \mathbf{v}_j \mathbf{v}_j^H \mathbf{h}_k} \right). \quad (5)$$

To ensure that every VU is able to decode the common data stream, the lowest common data stream channel capacity must be larger than the sum of VU's common stream decoding rate. Therefore, it has the rate limitation given by [1], [2]

$$\sum_{k=1}^U R_k^c \leq \min(c_k), \quad (6)$$

where  $\min(c_k)$  is the lowest common stream rate among all VUs,  $R_k^c$  is the common data rate allocated to  $k$ -th VU. Without loss of generality, we assume VU 1 has the lowest channel gain, the sum of common stream rate upper bound is given by [3]:

$$\min(c_k) = \log_2 \left( 1 + \frac{\mathbf{h}_1^H \mathbf{v}_0 \mathbf{v}_0^H \mathbf{h}_1}{\sigma_k^2 + \sum_{k=1}^U \mathbf{h}_1^H \mathbf{v}_k \mathbf{v}_k^H \mathbf{h}_1} \right). \quad (7)$$

### B. Problem Formulation

To evaluate the RSMA system performance, we apply WSR as the performance metric. Accordingly, the downlink RSMA WSR problem is formulated as:

$$\mathbf{P}_1 : \max_{\mathbf{v}_k, R_k^c} \text{WSR} = \sum_{k=1}^U f_k (R_k^c + R_k^p), \quad (8)$$

$$\text{s.t.} \quad \sum_{k=0}^U \mathbf{v}_k^H \mathbf{v}_k + P_c \leq P_{\max}, \quad (8a)$$

$$\sum_{k=1}^U R_k^c \leq \min(c_k), \quad (8b)$$

$$\text{Tr}(\mathbf{v}_k \mathbf{v}_k^H) \geq P_0, \quad (8c)$$

$$R_k^c \geq 0, \quad (8d)$$

where (8) is the original problem in which the objective is to maximum the system WSR.  $f_k$  is the weight for VU  $k$ ; (8a) sets the total power consumption to be lower than BS power  $P_{\max}$ , and  $P_c$  is fixed circuit power consumption; in (8b), it guarantees common stream can be decoded by every VU; constraint (8c) guarantees the VUs' private data transmission quality by setting beamformers power lower bound; (8d) ensures the existence of common stream.

### III. PROPOSED SOLUTION

In this section, we solve the original problem  $\mathbf{P}_1$  by the iterative FP algorithm [16]. Then, we design a problem with a penalty factor to match PGD updating requirement. By adding learnable parameters and applying PGD algorithm, we propose a FP based DU method to address the problem with low complexity and high robustness.

#### A. Fractional Programming

We apply the standard semi-definite relaxation (SDR) and let  $\mathbf{V}_k = \mathbf{v}_k \mathbf{v}_k^H$ . Besides, we define auxiliary variables:

$$z_k^* = (\sigma_k^2 + \sum_{j \neq k}^U \mathbf{h}_k^H \mathbf{V}_j \mathbf{h}_k)^{-1} \mathbf{h}_k^H \mathbf{v}_k. \quad (9)$$

$$z_0^* = (\sigma_k^2 + \sum_{k=1}^U \mathbf{h}_1^H \mathbf{V}_k \mathbf{h}_1)^{-1} \mathbf{h}_1^H \mathbf{v}_0, \quad (10)$$

Given initial feasible values for  $\mathbf{v}_k$ ,  $z_k^*$  and  $z_0^*$  would be constant. And we set  $\Phi_0 = 1 + 2\text{Re}\{\sqrt{\bar{z}_0} \mathbf{h}_1^H \mathbf{V}_0 \mathbf{h}_1 z_0\} - \bar{z}_0(\sigma_k^2 + \sum_{k=1}^U \mathbf{h}_1^H \mathbf{V}_k \mathbf{h}_1) z_0$  and  $\Phi_k = 1 + 2\text{Re}\{\sqrt{\bar{z}_0} \mathbf{h}_1^H \mathbf{V}_0 \mathbf{h}_1 z_0\} - \bar{z}_k(\sigma_k^2 + \sum_{j \neq k}^U \mathbf{h}_k^H \mathbf{V}_j \mathbf{h}_k) z_k$ . Then, from FP principle [16],  $\mathbf{P}_1$  can be equivalently transformed as

$$\mathbf{P}_2 : \max_{\mathbf{v}_k, R_k^c} \sum_{k=1}^U f_k(R_k^c + \log_2(\Phi_k)), \quad (11)$$

$$\text{s.t.} \quad \sum_{k=1}^U R_k^c \leq \log_2(\Phi_0), \quad (11a)$$

(8a), (8c), (8d),

It can be readily shown that given  $z_k^*$ ,  $\mathbf{P}_2$  is convex with respect to  $\mathbf{v}_k$  and  $R_k^c$ . Therefore, it can be solved by well-known toolbox, such as CVX [17]. Then  $z_k^*$  is updated by  $\mathbf{P}_2$ 's solution  $\mathbf{v}_k$ . This iterative algorithm is shown in **Algorithm 1**.

---

#### Algorithm 1 FP Beamforming for WSR optimization

---

**Require:**  $\mathbf{h}_k$ ,  $f_k$ ,  $P_0$ ,  $P_c$ ,  $P_{\max}$ , initial value of  $z_0$ ,  $z_k$ ,  $\mathbf{v}_0$ ,  $\mathbf{v}_k$  and  $R_k^c$ . Set counter  $j = 1$  and convergence precision  $\phi_p$ .

**while**  $|\text{WSR}_{j+1} - \text{WSR}_j| > \phi_p$  **do**

**Step 1** Update  $\mathbf{V}_k$  and  $\text{WSR}_j$  from  $\mathbf{P}_2$  with  $z_k^*$ ,  $z_k^*$ ,

**Step 2** Apply eigen decomposition on  $\mathbf{V}_k$  to obtain  $\mathbf{v}_k$ ,

**Step 3** Update each  $z_k^*$ ,  $z_0^*$  by (9) and (10),  $j = j + 1$ .

**end while**

---

#### B. Projection Gradient Descent with A Penalty Function

In this subsection, the PGD algorithm is introduced, which splits  $\mathbf{P}_2$  into two parts: the gradient descent on the objective function (unconstrained problem) and a projection to ensure all constraints are met. Since in PGD algorithm, the derivative is directly based on  $\mathbf{v}_k$  and  $\mathbf{v}_0$  instead of SDR variable  $\mathbf{V}_k$  and  $\mathbf{V}_0$ . However, simply dropping all constraints in  $\mathbf{P}_2$  will lead to no gradient updates for  $\mathbf{v}_0$ . Therefore, we first reformulate  $\mathbf{P}_2$  by adding a penalty function of constraint (8b) to the objective

function, which couples gradient with  $\mathbf{v}_0$ . The unconstrained problem then becomes:

$$\mathbf{P}_3 : \max_{\tilde{\mathbf{v}}_k, \tilde{R}_k^c} \mathcal{L} = \sum_{k=1}^U f_k \left( \tilde{R}_k^c + \log_2(\Phi_k) \right) - \lambda \left( \sum_{k=1}^U \tilde{R}_k^c - \log_2(\Phi_0) \right). \quad (12)$$

Here,  $\lambda > 0$  is the penalty factor. When PGD updates  $\mathbf{v}_k, \forall k$  in RSMA system,  $\mathbf{v}_0$  can be updated in each iteration with the penalty function given in  $\mathbf{P}_3$ . Therefore, based on the unconstrained convex optimization in  $\mathbf{P}_3$ , the beamformers and common data rate  $\tilde{\mathbf{v}}_k^{i+1}, \tilde{\mathbf{v}}_0^{i+1}, \tilde{R}_k^{c,i+1}$  can be updated by  $\mathbf{v}_k^i, \mathbf{v}_0^i, R_k^{c,i}$  following their gradient descent direction. The iterative steps are given in (13), respectively.

$$\begin{aligned} \tilde{R}_k^{c,i+1} &= R_k^{c,i} + \alpha_{1,k} \nabla R_k^{c,i}, \\ \tilde{\mathbf{v}}_0^{i+1} &= \mathbf{v}_0^i + \alpha_2 \nabla \mathbf{v}_0^i, \\ \tilde{\mathbf{v}}_k^{i+1} &= \mathbf{v}_k^i + \alpha_{3,k} \nabla \mathbf{v}_k^i, \end{aligned} \quad (13)$$

where  $i$  is  $i$ -th iteration step,  $\alpha_{1,k}$ ,  $\alpha_2$  and  $\alpha_{3,k}$  are fixed step size. And  $\nabla R_k^{c,i}, \nabla \mathbf{v}_0^i, \nabla \mathbf{v}_k^i$  are gradients (derivatives) of  $\mathcal{L}$  with respect to  $R_k^c, \mathbf{v}_0$ , and  $\mathbf{v}_k$  are given as

$$\nabla R_k^{c,i} = \frac{\partial \mathcal{L}}{\partial R_k^{c,i}} = f_k - \lambda, \forall k \neq 0, \quad (14)$$

$$\nabla \mathbf{v}_0^i = \frac{\partial \mathcal{L}}{\partial \mathbf{v}_0^i} = \frac{2\lambda \bar{z}_0^i \mathbf{h}_1}{\Phi_0^i \ln 2}, \quad (15)$$

$$\nabla \mathbf{v}_k^i = \frac{\partial \mathcal{L}}{\partial \mathbf{v}_k^i} = \left( \frac{\zeta_k^i}{\Phi_k^i} + \sum_{j \neq k}^U \frac{\beta_{j,k}^i}{\Phi_j^i} + \mathbf{o}_k^i \right), \forall k \neq 0, \quad (16)$$

where  $\zeta_k^i, \beta_{j,k}^i$  and  $\mathbf{o}_k^i$  are given as

$$\zeta_k^i = \frac{\partial (2\text{Re}\{z_j^i \mathbf{h}_j^H \mathbf{v}_j^i\})}{\partial \mathbf{v}_k^i \ln 2} = 2f_k \bar{z}_k^i \mathbf{h}_k / \ln 2, \quad (17)$$

$$\begin{aligned} \beta_{j,k}^i &= -\frac{\partial z_j^i (\sigma_k^2 + \sum_{l \neq j}^U \mathbf{h}_j^H \mathbf{v}_l^i \mathbf{v}_l^{i,H} \mathbf{h}_j)}{\partial \mathbf{v}_k^i \ln 2} \\ &= -2z_j^i \bar{z}_j^i f_j \mathbf{h}_j \mathbf{h}_j^H \mathbf{v}_k^i / \ln 2, \forall k \neq 0, \end{aligned} \quad (18)$$

$$\mathbf{o}_k^i = \frac{\partial \lambda \left( \sum_{k=1}^U -R_k^{c,i} + \log_2(\Phi_0^i) \right)}{\partial \mathbf{v}_k^i} = \frac{-2\lambda z_0^i \bar{z}_0^i \mathbf{h}_1 \mathbf{h}_1^H \mathbf{v}_k^i}{\Phi_0^i \ln 2}. \quad (19)$$

To guarantee the updated variables in the feasible region of the original problem, we employ a projection method to meet all constraints in  $\mathbf{P}_2$ . Hence, the projection algorithm for  $\tilde{\mathbf{v}}_k^i, \forall k \in \{0, 1, \dots, U\}$  is given as:

$$\begin{aligned} \mathbf{v}_k^{i+1} &= \frac{\tilde{\mathbf{v}}_k^{i+1}}{\|\tilde{\mathbf{v}}_k^{i+1}\|} \sqrt{a_k^*}, k = \{0, 1, \dots, U\}, \\ a_k^* &= \frac{\tilde{a}_k}{\sum_{k=0}^U \tilde{a}_k} (\mathbf{P}_{\max} - (U+1)\mathbf{P}_0) + \mathbf{P}_0, \\ \tilde{a}_k &= \max(\|\tilde{\mathbf{v}}_k^{i+1}\|_2^2, \mathbf{P}_0) - \mathbf{P}_0. \end{aligned} \quad (20)$$

The projection approach above bounds the beamformer power within feasible region without changing beamforming

direction. Moreover, the corresponding projection for  $\tilde{R}_k^{c,i+1}$  is given as

$$\begin{aligned} R_k^{c,i+1} &= \frac{\max(\tilde{R}_k^{c,i}, 0)}{\sum_{k=1}^U \tilde{R}_k^{c,i}} \min(c_k^{i+1}) \\ &= \frac{\max(\tilde{R}_k^{c,i}, 0)}{\sum_{k=1}^U \tilde{R}_k^{c,i}} \log_2 \left( 1 + \frac{\mathbf{h}_k^H \mathbf{v}_k^{i+1} \mathbf{v}_k^{i+1,H} \mathbf{h}_k}{\sigma_k^2 + \sum_{j \neq k}^U \mathbf{h}_k^H \mathbf{v}_j^{i+1} \mathbf{v}_j^{i+1,H} \mathbf{h}_k} \right). \end{aligned} \quad (21)$$

When the number of iteration approaches to infinity,  $R_k^{c*}$ ,  $k \in \{k | f_k = \max(f_1, f_2, \dots, f_U)\}$ , has asymptotic property to achieve upper bound,  $\min(R_k)$ , while other  $R_k^c = 0$ . Therefore, projection step for  $R_k^c$  is simplified as:

$$R_k^{i+1,c} = \begin{cases} \min(c_k^{i+1}), & \text{if } f_k = \max(f_1, f_2, \dots, f_U), \\ 0, & \text{otherwise.} \end{cases} \quad (22)$$

### C. PGD Based Deep Unfolding

However, the gradient updating step given in above PGD has poor convergence performance, particularly when the step size is small. Moreover, the penalty function given in  $\mathbf{P}_3$  even punishes objective function when the constraints are in feasible region. Therefore, in this subsection, we design a DU structure [11], by adding learnable parameters  $\theta$  into the PGD gradient updating part. These learnable parameters are trained to dynamically adjust weights for beamformers at each iteration, thereby can converge within few steps, which is much faster than PGD.

Essentially, the DU structure is designed to follow each iteration in PGD. The difference is that, DU introduces some learnable parameters which assign the weights for the terms in polynomials of  $\Pi_1$  and  $\Pi_2$  to update  $\mathbf{v}_0^i$  and  $\mathbf{v}_k^i$ . Specifically, in the  $n$ -th layer,  $\mathbf{v}_0$  and  $\mathbf{v}_k$  in (13) are reformulated as:

$$\tilde{\mathbf{v}}_0^{n+1} = \mathbf{v}_0^n + \Pi_1(\mathbf{v}_0^n), \quad (23)$$

$$\tilde{\mathbf{v}}_k^{n+1} = \mathbf{v}_k^n + \Pi_2(\mathbf{v}_k^n). \quad (24)$$

Here,  $\Pi_1(\mathbf{v}_0^n)$  and  $\Pi_2(\mathbf{v}_k^n)$  are the  $n$ -th layer for  $\mathbf{v}_0$  and  $\mathbf{v}_k$ , which are given as,

$$\Pi_1(\mathbf{v}_0^n) = \ln 2 (\phi \mathbf{w}_0^n) \frac{\nabla \mathbf{v}_0^n}{\lambda}, \quad (25)$$

$$\Pi_2(\mathbf{v}_k^n) = (\phi \mathbf{w}_k^n) \left[ \frac{\zeta_k^n}{\Phi_k^n}, \frac{\beta_{1,k}^n}{\Phi_1^n}, \frac{\beta_{2,k}^n}{\Phi_2^n}, \dots, \frac{\beta_{j,k}^n}{\Phi_j^n}, \dots, \frac{\beta_{U,k}^n}{\Phi_U^n}, \frac{\alpha_k^n}{\lambda} \right]$$

$$\left[ \eta_k^n, \eta_j^{n,1}, \eta_j^{n,2}, \dots, \eta_j^{n,j}, \dots, \eta_j^{n,U}, \eta_k^{n,p} \right]^T \ln 2, \forall k \neq 0, \forall j \neq k, \quad (26)$$

$$\phi = [f_1, f_2, \dots, f_U, P_0, P_{\max}], \quad (27)$$

where  $\phi$  is the environment pattern vector, which is spliced by weights  $f_k$  and power consumption  $P_{\max}, P_0$ . And the learnable parameters for each layer are

$$\theta^n = \{\mathbf{w}_0^{n,T}, \mathbf{w}_k^{n,T}, \eta_k^n, \eta_j^{n,k}, \eta_k^{n,p}\}, \quad (28)$$

where  $\mathbf{w}_0^n, \mathbf{w}_k^n \in \mathbb{R}^{(U+2) \times 1}$ ,  $\eta_k^{n,p}, \eta_j^{n,k}, \eta_k^n \in \mathbb{R}$ .

The designing of learnable parameters follows some schemes proposed in [18], [19], which add parameters on each term

in gradient polynomial to change the weights of updating in different directions. Besides, in this particular problem, the penalty function given above has penalty factor  $\lambda$ . If we consider the penalty factor as the Lagrangian multiplier, the training process can be considered as the regression problem for learnable parameter  $\eta_k^p$  to regress the Lagrangian multiplier value in each iteration step. The learnable parameter,  $\mathbf{W}_k$ , is applied to construct a linear transformation with  $\phi$ . This linear transformation provides a robust factor to make PGD be adaptive to  $f_k, P_0$  and  $P_{\max}$ . Therefore, the beamformers gradient descent is able to be accelerated specifically with  $\phi$ . DU algorithm is given as **Algorithm 2**. A graphic illustration of DU layers is shown in Fig. 1.

---

### Algorithm 2 Deep Unfolding for FP-based WSR Optimization

---

**Require:** Initialize fixed parameters, learnable parameters, and set the layer number  $N$ , batch size, epoch, learning rate for optimizer in backward propagation,

counter = 0,

**while** epoch – counter > 0 **do**

counter = counter + 1,

**For each batch data:**

**Forward Propagation Part:**

Initial beamformers randomly, then for each layer:

**Step 1** Update  $z_k$ , by (9); Update  $z_0$ , by (10),

**Step 2** Update  $\tilde{\mathbf{v}}_0$ , by (25); Update  $\tilde{\mathbf{v}}_k$ , by (26),

**Step 3** Update  $\mathbf{v}_k$  and  $\mathbf{v}_0$  by projection (20),

**Step 4** Update  $R_k^c$  by (22),

**Step 5** Output results  $\{\mathbf{v}_0, \mathbf{v}_k, R_k^c\}$ ,

**Forward Propagation ends**

**Backward Propagation Part:**

**Step 6** Calculate the loss given by (29),

**Step 7** Backward Propagation, update  $\theta$  and optimizer.

**Backward Propagation ends**

**end while**

---

Lastly, for this learning problem, the loss function is:

$$\text{Loss} = \frac{1}{QN} \sum_{q=1}^Q \sum_{n=1}^N \log_2(n+1) (\widehat{\text{WSR}}_{q,n} - \text{WSR}_{q,n}^*), \quad (29)$$

$$\widehat{\text{WSR}}_{q,n} =$$

$$\sum_{k=1}^U f_k^q (R_{k,q}^{c,n} + \log_2 \left( 1 + \frac{\mathbf{h}_{k,q}^H \mathbf{v}_{k,q}^n \mathbf{v}_{k,q}^{n,H} \mathbf{h}_{k,q}}{\sigma_{k,q}^2 + \sum_{j \neq k}^U \mathbf{h}_{k,q}^H \mathbf{v}_{j,q}^n \mathbf{v}_{j,q}^{n,H} \mathbf{h}_{k,q}} \right)), \quad (30)$$

where  $q$  is the  $q$ -th sample in  $Q$  samples batch.  $\text{WSR}^*$  is the ground truth WSR provided in dataset, generated by **Algorithm 1**. The log loss function is similar to the shape of the iterative step. As a result, loss function couples the relationships between last layer outputs and each layer outputs like iterative process in traditional algorithm. Besides, the loss function sets a connection between each layer and loss function output to prevent gradient vanishing.

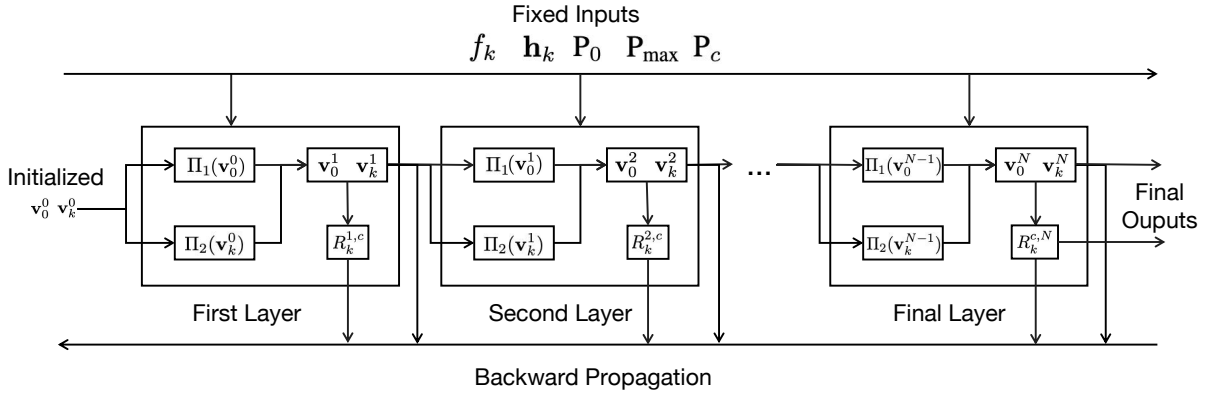


Fig. 1: Proposed Deep Unfolding Networks Structure Overview

#### IV. SIMULATION RESULTS

In this section, we evaluate the performance of proposed DU networks via numerical simulations. Firstly, we introduce the way to generate data set and training hyper-parameters. For experiments, the convergence evaluation and hyper-parameters evaluations are given to show which set of hyper-parameters gets the best results. Then, we test the robustness on OOD data set with different distributions of VUs' weights, high AWGN, and power lower bound. Finally, the complexity comparison is given to show the proposed algorithm has much faster computation speed than traditional algorithm.

In this work, we consider a scenario with  $U = 3$  VUs in downlink RSMA MISO system. The BS has  $M = 12$  antennas, and the maximum transmission power  $P_{\max} = 33$  dBm. The circuit power consumption  $P_c = 30$  dBm. Channel state information is represented as CSCG as mentioned above, where  $\mathbf{h}_k \sim \mathcal{CN}(0, 10\mathbf{I})$ ,  $n_k \sim \mathcal{N}(0, 1)$ . The convergence precision for FP IPM approach is  $\phi_p = 10^{-2}$ . The weights  $f_k$ , minimum power requirement of  $\mathbf{v}_k$  and AWGN power are stochastically generated following uniform distribution, i.e.,  $f_k \sim \mathcal{U}(0, 1)$  while  $\sum_{k=1}^U f_k = 1$ ,  $P_0 \sim \mathcal{U}(0, 0.125)$ . The dataset has 5969 samples generated by FP algorithm given in **Algorithm 1** with CVX tool box. Unless otherwise stated, we choose  $N = 12$ ,  $lr = 0.003$  as optimizer learning rate,  $bz = 1000$  as batch size, and  $ep = 80$  as epoch for the hyper-parameters setting.

##### A. Important Parameters Comparison and Effectiveness Test

In this subsection, we discuss the optimal hyper-parameter setting and evaluate network training effectiveness. Specifically, learning rate, batch size, and layer number are compared to find the best hyper-parameters and prove the effectiveness of the proposed method.

Fig. 2 shows the impact on the number of DU layers. The y-axis is the average sum ratio (ASR), defined as  $\frac{1}{Q} \sum_{q=1}^Q \frac{\widehat{WSR}_{q,N}}{WSR_{q,N}^*}$  that provides the average performance ratio of DU WSR and optimal WSR\*. When the ASR approaches to 1, the DU performance is closer to optimal results. As given by Fig. 2, the algorithm converges within few steps with relatively high performance, where ASR is near to 97% when layer

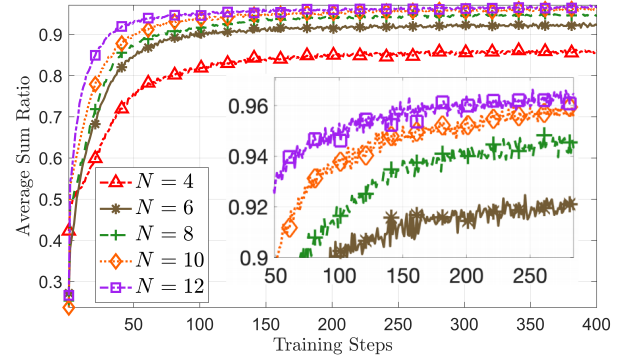


Fig. 2: Train Set Convergence Performance Comparison with Different Number of Layers

number is 12. Besides, when the number of layers increases, ASR continues to increase but the improvement becomes marginal after  $N = 8$ . In DU, each layer is constructed according to PGD iteration, which follows the iterative gradient descent process in optimization algorithm. As  $N$  grows, DU is also progressed to better results due to model convergence.

In Table I, DU's performance in test set is provided with different hyper-parameters, which maintains its generalization ability. This explains that although the DU is trained by a small data set, it can also converge rapidly to near-optimal results. The best ASR can reach over 97% with hyper-parameters:  $N = 12, lr = 0.003, bz = 200$ .

##### B. Out-of-distribution Test

In this subsection, the stricter generalizability test, OOD test, where we apply  $N = 12, lr = 0.003, bz = 1000$  as hyper-parameters setting. Since data-driven neural networks perform much worse in OOD [11], while model-driven is designed with explicit expression to adapt to various OOD scenarios. We test the generalizability on 3 OOD scenarios which are (Scenario 1) summation of weights summation less than 1; (Scenario 2) higher mean AWGN power scenario; (Scenario 3) scenario with different distribution of power lower bound  $P_0$ . In scenario 1, the summation of  $f_k$  follows uniform distribution  $\mathcal{U}(0, 1)$ . For the second scenario,  $\sigma_k^2 \sim \mathcal{N}(0.5, 4)$ , while the third

TABLE I: Important Parameters Comparison in Test Set Generalizability Performance

Parameters	Learning Rate Part Test Set Performance					Batch Size Part Test Set Performance				
	$lr = 0.015$	$lr = 0.01$	$lr = 0.005$	$lr = 0.003$	$lr = 0.001$	$bz = 200$	$bz = 400$	$bz = 700$	$bz = 1000$	$bz = 2000$
ASR (%)	96.77	<b>96.99</b>	96.78	96.71	95.18	<b>97.08</b>	96.88	96.66	96.71	95.36
Parameters	Layer Number Part Test Set Performance									
	$N = 4$		$N = 6$		$N = 8$	$N = 10$		$N = 12$		
ASR (%)	85.75		92.50		94.70	96.39		<b>96.71</b>		

scenario has  $P_0 \sim \mathcal{U}(0, 1/3)$ . Since the learnable parameters are restricted by the explicit expression computation in DU networks, the DU can maintain its performance in training set and learn the deeper mapping relationship underlying optimization rules. As shown in Table II, thanks to the model-based design, in OOD set, DU shows comparable ASR performance with baseline, which shows its strong resilience to a more general communication setting.

TABLE II: OOD Performance Results

Parameters	Baseline	Scenario 1	Scenario 2	Scenario 3
Special Distribution	None	$\mathcal{U}\{0, 1\}$	$\mathcal{N}(0.5, 4)$	$\mathcal{U}\{0, 1/3\}$
ASR (%)	96.71	91.55	96.21	97.72

### C. Complexity Comparison with FP-based Optimization

In this subsection, we provide computation efficiency comparison experiment to evaluate traditional optimization and proposed method complexity. To show the performance of proposed DU neural networks, we employ the value given by DU trained parameters from Python to MATLAB and setup a DU forward propagation structure with  $N = 12$  layers, and compare the execution time with FP algorithm given by CVX tool box. We repeat Monte Carlo experiments of FP and proposed DU for 20 times to obtain average results. The corresponding execution time (unit in second) is given in Table III. It is shown that the proposed DU method is 156 times faster than traditional FP-based optimization, a significant improvements on computation complexity. Therefore, this method well-suited for vehicular communication scenarios, where latency is a major performance metric.

TABLE III: Computation Time Comparison

Approach	FP-based Optimization	Proposed DU
Total Time	8.17392	<b>0.05232</b>
Time for Each Step/ Layer	2.04348	<b>0.00436</b>

## V. CONCLUSION

This paper focuses on the downlink WSR vehicular communication problem with RSMA. We aim to obtain the optimal beamforming vectors for each VU. By applying a well-designed penalty function, we proposed an FP and PGD based DU neural network framework, which shows comparable performance with traditional optimization approach but with much lower complexity. This paper provided extensive numerical results and has shown the advantages of proposed method in ASR, OOD, and computation time performance.

## REFERENCES

- [1] B. Clerckx, Y. Mao, E. A. Jorswieck, J. Yuan, D. J. Love, E. Erkip, and D. Niyato, "A primer on rate-splitting multiple access: Tutorial, myths, and frequently asked questions," *IEEE Journal on Selected Areas in Communications*, 2023.
- [2] B. Clerckx, H. Joudeh, C. Hao, M. Dai, and B. Rassouli, "Rate splitting for mimo wireless networks: A promising phy-layer strategy for lte evolution," *IEEE Communications Magazine*, vol. 54, no. 5, pp. 98–105, 2016.
- [3] Z. Yang, M. Chen, W. Saad, and M. Shikh-Bahaei, "Optimization of rate allocation and power control for rate splitting multiple access (rsma)," *IEEE Transactions on Communications*, vol. 69, no. 9, pp. 5988–6002, 2021.
- [4] Z. Yang, M. Chen, W. Saad, W. Xu, and M. Shikh-Bahaei, "Sum-rate maximization of uplink rate splitting multiple access (rsma) communication," *IEEE Transactions on Mobile Computing*, vol. 21, no. 7, pp. 2596–2609, 2020.
- [5] M. Xiao, H. Cui, Z. Zhao, X. Cao, and D. O. Wu, "Joint 3d deployment and beamforming for rsma-enabled uav base station with geographic information," *IEEE Transactions on Wireless Communications*, 2023.
- [6] O. Dizdar, A. Sattarzadeh, Y. X. Yap, and S. Wang, "Rsma for overloaded mimo networks: Low-complexity design for max-min fairness," *IEEE Transactions on Wireless Communications*, 2023.
- [7] B. Clerckx, Y. Mao, Z. Yang, M. Chen, A. Alkhateeb, L. Liu, M. Qiu, J. Yuan, V. W. Wong, and J. Montojo, "Multiple access techniques for intelligent and multi-functional 6g: Tutorial, survey, and outlook," *arXiv preprint arXiv:2401.01433*, 2024.
- [8] Q. Zhang, L. Zhu, S. Jiang, and X. Tang, "Deep unfolding for cooperative rate splitting multiple access in hybrid satellite terrestrial networks," *China Communications*, vol. 19, no. 7, pp. 100–109, 2022.
- [9] J. Gao, C. Zhong, G. Y. Li, and Z. Zhang, "Online deep neural network for optimization in wireless communications," *IEEE Wireless Communications Letters*, vol. 11, no. 5, pp. 933–937, 2022.
- [10] L. Zhang, H. Sun, J. Sun, R. Parasuraman, Y. Ye, and R. Q. Hu, "Map2schedule: An end-to-end link scheduling method for urban v2v communications," 2023.
- [11] N. Shlezinger, J. Whang, Y. C. Eldar, and A. G. Dimakis, "Model-based deep learning," *Proceedings of the IEEE*, 2023.
- [12] L. Schynol and M. Pesavento, "Coordinated sum-rate maximization in multicell mu-mimo with deep unrolling," *IEEE Journal on Selected Areas in Communications*, vol. 41, no. 4, pp. 1120–1134, 2023.
- [13] J. Zhang, C. Masouros, and L. Hanzo, "Joint precoding and csi dimensionality reduction: An efficient deep unfolding approach," *IEEE Transactions on Wireless Communications*, 2023.
- [14] J. Gallier and J. Quaintance, "Fundamentals of optimization theory with applications to machine learning," *University of Pennsylvania Philadelphia, PA*, vol. 19104, 2019.
- [15] W. Xia, Y. Jiang, B. Zhao, H. Zhao, and H. Zhu, "Deep unfolded fractional programming based beamforming in ris-aided miso systems," *IEEE Wireless Communications Letters*, 2023.
- [16] K. Shen and W. Yu, "Fractional programming for communication systems—part i: Power control and beamforming," *IEEE Transactions on Signal Processing*, vol. 66, no. 10, pp. 2616–2630, 2018.
- [17] M. Grant and S. Boyd, "Cvx: Matlab software for disciplined convex programming, version 2.1," 2014.
- [18] N. Samuel, T. Diskin, and A. Wiesel, "Learning to detect," *IEEE Transactions on Signal Processing*, vol. 67, no. 10, pp. 2554–2564, 2019.
- [19] N. T. Nguyen and K. Lee, "Deep learning-aided tabu search detection for large mimo systems," *IEEE Transactions on Wireless Communications*, vol. 19, no. 6, pp. 4262–4275, 2020.